Biocatalysis, Protein Engineering, and Nanobiotechnology **Biotechnology and Bioengineering**

DOI 10.1002/bit.26503

N-glycan engineering of a plant-produced anti-CD20-hIL-2 immunocytokine significantly enhances its effector functions. †

Running Title: Immunocytokine with enhanced effector functions.

Carla Marusic[1,*], Claudio Pioli[2,*], Szymon Stelter[3], Flavia Novelli[2], Chiara Lonoce[1], Elena Morrocchi[2], Eugenio Benvenuto[1], Anna Maria Salzano[4] , Andrea Scaloni[4], and Marcello Donini[1]

[1]Laboratory of Biotechnology; ENEA Research Center Rome, Italy

[2]Laboratory of Biomedical Technologies, ENEA Research Center Rome, Italy

[3]Molecular Immunology Unit, Institute for Infection and Immunity, St. George's University of London, London, UK

[4]Proteomics & Mass Spectrometry Laboratory, ISPAAM, National Research Council, 80147 Napoli, Italy

[*] These authors have contributed equally to this work.

Corresponding author: marcello.donini@enea.it
Tel. +39 06 3048 4151, Fax +39 06 30484808
Laboratory of Biotechnology, ENEA Research Center
Via Anguillarese 301
00123, Roma, Italy

[†]This article has been accepted for publication and undergone full peer review but has not been through the copyediting, typesetting, pagination and proofreading process, which may lead to differences between this version and the Version of Record. Please cite this article as doi: [10.1002/bit.26503]

Additional Supporting Information may be found in the online version of this article.

Received October 9, 2017; Revision Received November 17, 2017; Accepted November, 20, 2017

Abstract

Anti-CD20 recombinant antibodies are among the most promising therapeutics for the treatment of B-cell malignancies such as non-Hodgkin lymphomas. We recently demonstrated that an immunocytokine (2B8-Fc-hIL2), obtained by fusing an anti-CD20 scFv-Fc antibody derived from C2B8 mAb (rituximab) to the human interleukin 2 (hIL-2), can be efficiently produced in *Nicotiana benthamiana* plants. The purified immunocytokine (IC) bearing a typical plant protein N-glycosylation profile showed a CD20 binding activity comparable to that of rituximab and was efficient in eliciting antibody-dependent cell-mediated cytotoxicity (ADCC) of human PBMC against Daudi cells, indicating its fuctional integrity. In this work, the immunocytokine devoid of the typical xylose/fucose N-glycosylation plant signature (IC-ΔXF) and the corresponding scFv-Fc-ΔXF antibody not fused to the cytokine, were obtained in a glyco-engineered ΔXylT/FucT *N. benthamiana* line. Purification yields from agroinfiltrated plants amounted to 20-35 mg/Kg of leaf fresh weight. When assayed for interaction with FcγRI and FcγRIIIa, IC-ΔXF exhibited significantly enhanced binding affinities if compared to the counterpart bearing the typical plant protein N-glycosylation profile (IC) and to rituximab. The glyco-engineered recombinant molecules also exhibited a strongly improved ADCC and complement-dependent cytotoxicity (CDC). Notably, our results demonstrate a reduced C1q binding of xylose/fucose carrying IC and scFv-Fc compared to versions that lack these sugar moieties. These results demonstrate that specific N-glycosylation alterations in recombinant products can dramatically affect the effector functions of the immunocytokine, resulting in an overall improvement of the biological functions and consequently of the therapeutic potential.

Keywords: Molecular farming; Immunocytokine; N-glycosylation; non-Hodgkin lymphoma; Complement-dependent cytotoxicity; Fcγ receptors.

1. Introduction

Non-Hodgkin lymphomas (NHLs) are a group of solid tumors originating from lymphocytes at different developmental stages, representing a major health problem for both developed and developing countries (Perry et al., 2016). It has been estimated that 72,580 new cases of non-Hodgkin Lymphoma were diagnosed in 2016 in the USA (Armitage et al., 2017). Most NHLs' express the leukocyte antigen CD20, a transmembrane glycoprotein that is the target of the anti-CD20 antibody rituximab (C2B8), which represents the first recombinant antibody used to cure B-cell lymphomas (Reff et al., 1994; Calcagno et al., 2012). However, a durable anti-cancer response with rituximab is rare, with many patients experiencing a relapse (Davis et al., 2014). Therefore, it is necessary to obtain new anti-CD20 antibodies engineered to improve their therapeutic activity against B-cell lymphomas by enhancing antibody-dependent cell-mediated cytotoxicity (ADCC) and complement-dependent cytotoxicity (CDC) (Sawas et al., 2017). In the last decade a new class of recombinant antibodies called 'immunocytokines', derived from the fusion of an antibody to a cytokine, proved to be very effective against several forms of tumors (Sondel and Gillies, 2012; Vincent et al., 2014). Major clinical successes have been obtained by fusing tumor targeting antibodies to the human interleukin 2 (hIL-2) (List and Neri, 2013). Immunocytokines based on IL2 fusion have shown a far better anti-cancer activity if compared to the individual administration of antibody and IL2 in combination therapies (Gubbels et al., 2011; Pretto et al., 2014; Fournier et al., 2011). In particular, an anti-CD30 antibody fused to two different cytokines (IL2 and IL12) showed an enhanced NK cells activation in a Hodgkin lymphoma mouse model (Jahn et al., 2012).

We recently described the plant production of an immunocytokine constructed as a protein fusion using the rituximab antibody scaffold and the hIL-2. The purified dimeric 2B8-Fc-hIL2 displayed a full biological activity for both antibody and cytokine components, as revealed by CD20 binding and induction of ADCC and by stimulation of proliferation in an IL-2-dependent cell line, respectively (Marusic et al., 2016). As expected, glycopeptide analysis showed a highly

homogeneous plant-type glycosylation with the presence of β1,2 xylose and α1,3 fucose, which may represent an unwanted feature of this plant-made antibody in cancer therapy. In recent years, one of the novel advantageous features of producing biopharmaceuticals in plants is the possibility to produce tailored made therapeutic glycoproteins by engineering the plant glycosylation pathway (Stoger et al., 2014). There are many evidences showing that certain glycan moieties may modify antibody functions (Jefferis, 2012; Qiu et al., 2014; Forthal et al., 2010). For this reason, there is a wealth of literature reporting glyco-engineering studies aimed at obtaining plants with human-type glycosylation patterns (Strasser et al., 2014). A milestone was the removal of plant-typical fucose and xylose residues through T-DNA insertional mutagenesis in *Arabidopsis thaliana* (Strasser et al., 2004) or by RNA interference approaches, as reported in duckweed (*Lemna minor*) (Cox et al., 2006), and ΔXylT/FucT *N. benthamiana* transgenic line (Strasser et al., 2008). As an example, a glyco-modified tumor-targeting immunoglobulin, (anti-CD30 monoclonal antibody) produced in *Lemna minor* silenced for the expression of the fucosyl- and xylosyl-transferase genes, showed an improved ADCC activity, if compared to the 'mammalian'-glycosylated cognate molecule (Cox et al., 2006).

In this study, we have expressed the anti-CD20 immunocytokine (IC-ΔXF) as well as the scFv-Fc-ΔXF antibody not fused to the IL2 in a ΔXylT/FucT *N. benthamiana* transgenic line (Strasser et al., 2008). Glycan analysis confirmed the homogeneous $GlcNAc_2Man_3GlcNAc_2$ glycosylation of both recombinant molecules, lacking xylose and fucose residues. The binding activity of these molecules to $CD20^+$ Daudi cells was comparable to that of the original rituximab. Notably, the IC-ΔXF immunocytokine possessed an improved binding to FcγRI and FcγRIIIa. This is coincident with an improved ADCC compared to their 'wild-type' plant-glycosylated counterparts as well as to rituximab. Intriguingly, we also observed a restored binding capacity to C1q, which matched to the significantly enhanced CDC activity.

2. Materials and Methods

2.1 Expression of recombinant molecules in ΔXylT/FucT *N. benthamiana*

Glycoengineered ΔXylT/FucT *N. benthamiana* plants, in which a targeted down-regulation of the endogenous beta1,2-xylosyltransferase (XylT) and alpha1,3-fucosyltransferase (FucT) encoding genes was obtained by RNA interference (RNAi) technology (Strasser et al., 2008), were kindly provided by Prof. Herta Steinkellner (University of Natural Resources and Life Sciences, Vienna, Austria). Plants were grown in an environmentally contained greenhouse at 25 °C under a 16-h light/8-h dark photoperiod. Transient expression of the glyco-engineered molecules was performed essentially as previously reported by Marusic and colleagues (Marusic et al., 2016). Briefly, bacterial cultures (*A. tumefaciens* -LBA 4404- clones carrying IC, scFv-Fc or P19 expression vectors) were centrifuged at 4,000 *g* and resuspended in MES buffer for infiltration (10 mM MES, 10 mM $MgSO_4$, pH 5.8). Agrobacterium suspensions were mixed (IC and p19 or scFv-Fc and p19) reaching final optical density (OD_{600}) of 0.5 for each culture and used to vacuum-infiltrate ΔXylT/FucT *N. benthamiana* plants (at the 6-7 leaf stage). Agroinfiltrated leaves were collected at 4 days post-infiltration obtaining batches of 40 g of leaves and stored at -80 °C.

2.2 Purification and size exclusion chromatography (SEC)

Purification of anti-CD20 recombinant molecules was performed from batches of 40 g of agroinfiltrated ΔXylT/FucT *N. benthamiana* leaves by protein A affinity chromatography as previously described by Marusic and colleagues (Marusic et al., 2016). Briefly, homogenized leaves (in a PBS volume of 80 ml, 0.2% Tween, Complete™ Roche protease inhibitor cocktail) were clarified by centrifugation and filtration through a 0.45μm syringe filter (Millex-HP Syringe Filter, Millipore), the supernatant was loaded on protein A affinity column (1 ml HiTrap™ Protein A FF, GE Healthcare) following manufacturer instructions. SEC of purified proteins was performed using a calibrated SuperdexTM 200 5/150 GL column (GE Healthcare). Elution was performed in PBS using a 0.3 ml/min flow rate on an ÄKTA FPLC P920 instrument (GE Healthcare) at 20 °C, as

previously reported (Lombardi et al., 2010). Absorbance was measured at 280 nm and expressed as Absorption Units (mAU). Calibration of the column was achieved using gel filtration calibration kits (Low and High Molecular Weight GE Healthcare). The commercial CHO-derived rituximab was also used as a control.

2.3 Immunocytokine expression analysis

To verify the presence of the hIL-2 fusion domain in IC-ΔXF, the purified immunocytokine at a concentration of 500 ng/mL was used in ELISA assays. The purified scFv-Fc-ΔXF antibody at the same concentration was used as a negative control. Nunc-Immuno Maxisorp wells were coated with an anti-human γ chain antibody (I6010, Sigma-Aldrich). Blocking of the ELISA plate was performed in PBS with 2% milk (w/v). The anti-hIL-2 (Cell Signaling Technology®, D7A5, USA) at the dilution of 1:1,000 was used for detection, followed by an HRP-conjugated anti-rabbit antibody (0545, Sigma) diluted 1:10,000. To assay binding to C1q, ELISA plates were incubated with serial dilutions of the purified recombinant molecules (starting from a concentration of 10 µg/mL) in carbonate-bicarbonate buffer (50mM $Na_2CO3/NaHCO_3$, pH 9.6). Blocking was performed using 1% BSA. The Complement component C1q from human serum (C1740, Sigma) was added to the wells at a concentration of 2µg/mL. The HRP-conjugated anti-C1q antibody (Abcam, ab46191) diluted 1:400 was used for detection. Determination of HRP activity was performed using a microtitre plate reader at 405 nm (TECAN-Sunrise). The 2,2-azino-di-3-ethylbenz-thiazoline sulphonate (ABTS, KPL) was used as reagent. Analysis of purified products was performed by SDS-10% PAGE under reducing and non-reducing conditions and protein bands were stained with Coomassie blue. The commercial CHO-derived rituximab (hcd20-mab1, Invivogen, San Diego CA, USA) was used as a control as well as a protein molecular mass marker (Color burst™, C1992 Sigma).

2.4 Analysis of protein N-glycosylation

The IC-ΔXF, scFv-Fc-ΔXF and scFv-Fc molecules were subjected to SDS-PAGE under reducing conditions and corresponding bands were excised, extracted with 25 mM NH_4HCO_3/acetonitrile (1:1 v/v), processed and digested with trypsin (Roche) (D'Ambrosio et al., 2008). Glycopeptides were enriched and analysed as described by Marusic and colleagues (Marusic et al., 2016). Briefly, capillary NuTip Gel loader HILIC columns (Glygen, Columbia, MD) were used to obtain glycopeptides enriched fractions that were subsequently subjected to MALDI-TOF-MS analysis. 2,5-dihydroxy-benzoic acid (10 mg/mL in 50% v/v acetonitrile, 0.1% v/v trifluoroacetic acid) was used as ionization matrix, and mass spectra were acquired on a Bruker Ultraflextreme MALDI-TOF-TOF instrument (Bruker Daltonics), in reflectron mode in *m/z* range 500-5000. Acquired mass spectra were analysed using FlexAnalysis software (Bruker Daltonics); GPMAW 4.23 software (Lighthouse Data, Denmark) was used for the assignment of mass signals based on the amino acid sequence of the antibody constructs. Searching parameters were set to consider trypsin, a missed cleavages maximum value of 2, Cys carbamidomethylation and Met oxidation and N-terminal Glu/Gln cyclization as variable modifications, respectively. A 0.02% mass tolerance value was used to match mass values to protein regions. Glycopeptide assignment by MALDI LIFT-TOF/TOF-MS was verified by manual spectral inspection.

2.5 Flow cytometry

Binding of glycoengineered molecules to CD20 was assayed using $CD20^+$ Daudi cells (ATCC, code CCL213). Cells were incubated with the different molecules (rituximab, IC, IC-ΔXF, scFv-Fc or scFv-Fc-ΔXF) and an unrelated plant derived anti-tenascin C mAb H10 (Villani et al., 2009). CD20 receptor binding was assayed with a goat anti-human IgG polyclonal Ab (Invitrogen H10700), and a fluorescein isothiocyanate (FITC)-conjugated rabbit anti-goat IgG polyclonal Ab (Sigma Aldrich F7367). A FACSCalibur (BD Biosciences) was used to collect fluorescence signals in log mode.

2.6 Immunocytokine kinetics and affinity for FcγRI and FcγRIIIa.

Surface plasmon resonance experiments were performed on a Biacore X100 (GE Healthcare). First, Protein A sensor chip was prepared by immobilizing soluble Protein A from *Staphylococcus aureus* recombinantly expressed in *E. coli* (Sigma) on a CM5 sensor chip (GE Healthcare) by amine-coupling. A 1:1 mixture of 0.1 M NHS (N-hydroxysuccinimide) and 0.1 M EDC (3-(N,N-dimethylamino) propyl-N-ethylcarbodiimide) was injected for 7 min at a flow rate of 5 µl/min, followed by injection of 25 µg/ml Protein A in 10 mM sodium acetate, pH 4.5, on both flow cells until 3500 RU (Resonance Units) target was reached. The surface was blocked with 1 M ethanolamine-HCl pH 8.5. For kinetics and affinity measurements recombinant molecules were captured on flow cell 2 of the Protein A sensor chip to a level of 210 RU or 290 RU (for FcγRI or FcγRIIIa analysis respectively). The flow cell 1 served as a reference surface. Recombinant ectodomains of human FcγRI or high affinity variant FcγRIIIa-V158 (R&D SYSTEMS MN, USA) were injected into both flow cells at the flow rate 40 µl/min and Protein A surface was regenerated with 10 mM glycine-HCl pH 1.5. Binding of human FcγRI (31.4 kDa) was observed at five two-fold dilutions starting at 30 nM, with binding time 135s and dissociation of 600s. For FcγRIIIa (22.6 kDa) the tested concentrations were 2 µM, 1 µM, 0.5 µM, 0.25 nM and 0.125 µM (IC) and 800 nM, 400 nM, 200 nM, 100nM, 50 nM, 25 nM, 12.5 nM (IC-ΔXF). The analysis was performed in running buffer 10 mM HEPES, 150 mM NaCl, 0.005% P20, pH 7.4 at 25°C. Sensorgrams were corrected using double referencing procedure – subtracting responses from the reference surface and from zero concentration of the analyte. The data were analyzed with 1:1 binding model, or two-state reaction model for the FcγRIIIa–anti-HBsAg interaction, using the global data analysis option available within Biacore X100 Evaluation 2.0.1 software.

2.7 Antibody-dependent cell-mediated cytotoxicity and Complement dependent cytotoxicity

The lactate dehydrogenase (LDH) release assay was used to evaluate ADCC employing IL-2-activated human PBMCs as effector cells (E) and Daudi cells as target cells (T) at an E:T ratio of

25:1. PBMCs obtained from healthy donors blood by discontinuous gradient centrifugation (Histopaque1077; Sigma Aldrich) were stimulated for 18 hours with IL-2 at 20 ng/ml (cat H7041; Sigma Aldrich, Saint Louis, MO), at 37°C in a humidified, 5% CO_2 atmosphere. Target cells (10^4/well) were incubated with the anti-hCD20-hIgG1 mAb (RTX) at 10 μg/ml or the plant-derived recombinant molecules at equimolar concentrations in culture plates (96-well U-bottomed). An irrelevant plant-derived antibody (F8-Fc) was used as negative control (Capodicasa et al., 2011). IL-2-activated PBMCs were added ($2.5x10^5$/well) after 30 min and LDH release was evaluated after an incubation of 4 h (Cat. G1780, Promega, Madison, WI). Calculation of cytotoxic lysis (%) was performed as follows: 100x(experimental release-spontaneous release)/(maximal release-spontaneous release). For the CDC assay, highly viable (>95%) exponentially growing Daudi cells were seeded ($5x10^5$ cells/tube) in complete medium with serial dilutions (35-140 nM) of either IC, IC-ΔXF or scFv-Fc, scFv-Fc-ΔXF and rituximab. Human serum from healthy donors was used as source of complement. Samples with cells and human serum or the recombinant molecules alone were also used as controls. Cells were incubated at 37°C and 5% CO_2 for 30 min and after washing were stained with propidium iodide (PI) for 5 min at room temperature and analyzed by flow cytometry. Results were expressed as the percentage of dead cells positively stained by PI.

2.8 IL-2-dependent cell proliferation

The assay was essentially performed as described before by Marusic and colleagues (Marusic et al., 2016). Briefly, CTLL-2 cells were incubated without hIL-2 and then transferred in 96 well plates ($2.5x10^5$/ml) and cultured again with complete medium alone or stimulated for 48 h with 160nM of IC, IC-ΔXF, scFv-Fc, scFv-Fc-ΔXF, rituximab or rhIL-2 as a control. The 490 nm absorbance was measured by an ELISA microtitre plate reader (TECAN-Sunrise) after adding (20 μl/well) Cell Titer 96TM Aqueous one solution (Promega G3580).

2.9 Statistical analysis

Comparison of groups was perfomed using One-way ANOVA and for unpaired samples, a Bonferroni-corrected two-tailed Student t-test was also applied. To compare groups for proportions a χ^2 test was used. In the figure legends significance levels are shown; p values < 0.05 were considered statistically significant.

3. Results

3.1 Purification and biochemical characterisation of the immunocytokine produced in ΔXylT/FucT *N. benthamiana*

Purification of recombinant molecules from vacuum-agroinfiltrated ΔXylT/FucT *N. benthamiana* plants was performed starting from 40 g of leaf fresh weight (FW). Clarified supernatants obtained from mechanical homogenisation extraction were directly loaded onto a protein A affinity chromatography column. Typical yield for IC-ΔXF and scFv-Fc-ΔXF was 20 mg/kg (FW) and 35 mg/kg FW, respectively. Analysis of the proteins by SDS-PAGE was performed in reducing and non-reducing conditions is shown in Figure 1A, B. Under non-reducing conditions, a major band of about 130 kDa was observed for both IC-ΔXF and IC, (Figure 1A, lanes 2 and 3) while the expected band at a slightly lower molecular mass was reported for scFv-Fc-ΔXF and scFv-Fc (Figure 1A, lanes 4 and 5), both consistent with the fully assembled recombinant products. All samples also displayed additional very faint components migrating at a lower mass value of ~100 kDa and ~60 kDa, probably corresponding to degradation products. It must be noted that there is no difference in band profiles and intensity between glycoengineered and non-glycoengineered molecules of the same format. As a control, the CHO derived rituximab was used (Figure 1A, lane 1). Analysis under reducing conditions revealed bands of the expected size, plus a very faint degradation product at about 30 kDa (Figure 1B). Purified molecules were also subjected to size-exclusion chromatography in order to characterize their molecular assembly and integrity. Analysis showed that ~ 90% of the purified products (IC and IC-ΔXF) (Fig. 1C, bottom panels) had the

expected molecular mass of about 130 kDa, consistent with the major peak eluting at 2.10 ml. As expected, the CHO derived rituximab (~ 150 kDa) used as a control, showed a major peak at 2.08 ml (Fig. 1b, top panel). Other two minor peaks eluting at about 2.54 ml and 2.89 ml were also specifically observed in IC and IC-ΔXF consistent with the presence of lower molecular mass fragments that were also revealed in non-reducing SDS-PAGE analysis (Fig. 1A). Analysis of scFv-Fc and scFv-Fc-ΔXF revealed that about 95 % of the purified antibodies had the expected molecular mass, which corresponded to a major peak eluting at about 2.12 ml. Also in this analysis no significant differences were reported in the chromatographic profiles between glycoengineered and non-glycoengineered molecules of the same format. The presence of the hIL-2 domain was assessed in ELISA using an anti-hIL-2 antibody. In Figure 1D the purified IC-ΔXF shows an intense immunoreactivity, while the scFv-Fc-ΔXF control displays no significant reaction.

3.2 Glycosylation analysis of the anti-CD20 immunocytokine

Glycosylation of the IC-ΔXF and scFv-Fc-ΔXF recombinant molecules was compared in MALDI-TOF-MS experiments to that of the scFv-Fc, which was previously demonstrated (Marusic et al., 2016) as bearing a typical plant-type protein N-linked glycosylation moiety containing xylose and fucose residues (Figure 2). In fact, the corresponding tryptic digest, which was further subjected to hydrophilic interaction liquid chromatography (HILIC) for glycopeptide trapping, showed an intense MH^+ signal, corresponding to the singly protonated species generated in the ionization process, at about *m/z* 2766.041 (Figure 2A). This signal was associated with the glycosylated peptide EEQYNSTYR (339-347) showing a complex-type N-linked glycan structure, *i.e.* $GlcNAc_2Man_3(Xyl)(Fuc)GlcNAc_2$ (Fuc, fucose; GlcNAc, N-acetylglucosamine; Man, mannose; Xyl, xylose). A low intensity peak at *m/z* 2619.967 was also detected, which was probably generated from glycan fragmentation reactions during MALDI-TOF-MS analysis (Marusic et al., 2016). The MH^+ signal at about *m/z* 2766.041 was completely absent in the case of the HILIC

fractions from IC-ΔXF and scFv-Fc-ΔXF digested with trypsin, which conversely showed the occurrence of prominent MH^+ peaks at *m/z* 2487.869 and 2487.757 (Figure 2B and C). The latter were further assigned by MALDI LIFT-TOF/TOF-MS experiments, which demonstrated their nature as related to the peptide EEQYNSTYR bearing, in this case, a $GlcNAc_2Man_3GlcNAc_2$ glycan moiety (Supplementary Figure S1). Minor MH^+ signals related to the above-mentioned glycan fragmentation reactions were also observed for IC-ΔXF and scFv-Fc-ΔXF. The small peptide species at m/z 2469.854 and 2469.723 (Fig. 2B and C) were associated to a modified form of the most abundant glycopeptide, which occurs at 2487.869 and 2487.757, respectively. They originated from a cyclization process generating a pyroglutamic acid (instead of glutamic acid) at the N-terminal position. On the other hand, we verified that no signals corresponding to the non-glycosylated peptide EEQYNSTYR or related peptides were observed either following MALDI-TOF-MS and nLC-ESI-LIT-MS/MS analysis of the tryptic digests of all recombinant proteins before their HILIC enrichment step (data not shown); the latter analysis was performed as previously described (Marusic et al., 2016). This led us to conclude that either the recombinant proteins are fully glycosylated or contains undetectable traces of the non-glycosylated counterparts. In the whole, above-mentioned results demonstrated that by using the ΔXylT/FucT *N. benthamiana* expression system we obtained recombinant products whose N-linked glycosylation pattern is highly homogeneous with a largely dominant glycoform (>95%) lacking core xylose and fucose residues.

3.3 Immunocytokine kinetics and affinity for FcγRI and FcγRIIIa.

To verify whether the presence of human IL2 fused to the heavy chain C-terminus affects the interaction of Fc region with FcγRs, and how glyco-engineering modulates this interaction, kinetic measurements using surface plasmon resonance (SPR) were performed. Binding to the FcγRs of the glyco-engineered IC-ΔXF was compared to rituximab and to IC. The results demonstrated that IC formed less stable complexes with FcγRI, characterized by faster dissociation and consequently

10-fold lower affinity than rituximab (Figure 3A, Table 1). However, IC-ΔXF showed similar binding pattern to FcγRI as rituximab, with slightly increased affinity (150 pM as compared to 332 pM of rituximab). Since both IC and IC-ΔXF bear the IL2 fusion and the only difference is determined by glycosylation pattern, this suggests that the impaired binding observed for IC is mostly due to glycosylation rather than IL2 fusion to Fc region. Similarly, IC could not engage effectively the FcγRIIIa (Figure 3B). Low binding responses observed did not allow precise affinity measurements and indicate either very low affinity (>2μM) or a presence of inactive population that is not able to engage the receptor. In contrast, the glyco-engineered IC-ΔXF demonstrated 15-fold higher affinity (23.6 nM) to FcγRIIIa than rituximab (377 nM) (Table 2).

3.4 Biological activity of the anti-CD20 immunocytokine

CD20 binding and Antibody-dependent cell-mediated cytotoxicity

The functional integrity of the recombinant molecules was assessed verifying their ability to bind to CD20 (Fab integrity) and to be recognized by Fc receptors eliciting functional responses (Fc integrity). Binding to CD20 expressed on Daudi cells was assessed by flow cytometry comparing glyco-engineered IC-ΔXF and scFv-Fc-ΔXF to the counterparts produced in "wild-type" plants. Results showed no statististically significant difference of antigen-binding as revealed by percentage of positive cells, indicating that glyco-engineering did not affect the antigen-binding function of the recombinant molecules (Figure 4). To assay the capacity of IC-ΔXF and scFv-Fc-ΔXF to induce effector functions we performed an ADCC assay using IL-2-activated human peripheral blood mononuclear cells (PBMC) as a source of effector cells and Daudi cells as a source of target cells. Rituximab as well as IC and scFv-Fc were used for comparison but also to set-up the optimal concentration conditions and effector to target cell ratio. Target cell lysis was assayed by lactate dehydrogenase (LDH) release. Results revealed that both IC-ΔXF and scFV-Fc-ΔXF are capable of inducing an ADCC response, producing a significantly higher percentage of cell lysis

compared to that of rituximab and the 'wild-type' plant-glycosylated IC and scFv-Fc molecules (Figure 5A).

Human C1q binding, CDC and IL2 activity

Binding of the glyco-modified immunocytokine to the human component C1q was assayed by ELISA. Results showed that, whereas the 'wild-type' plant-glycosylated molecules exhibited a barely detectable binding, both IC-ΔXF and scFv-Fc-ΔXF bound very efficiently to C1q. Noteworthy, both IC-ΔXF and scFv-Fc-ΔXF bound C1q more efficiently than rituximab, confirming that the glyco-engineering rendered their sites of interaction with C1q readily accessible (Figure 5B). The capacity of IC-ΔXF and scFv-Fc-ΔXF to mediate CDC was assayed on Daudi cells using human serum as source of complement proteins. Results demonstrated that IC and scFv-Fc produced in 'wild-type' plants were not able to induce lysis of Daudi cells, paralleling findings on C1q binding. Conversely, both IC-ΔXF and scFv-Fc-ΔXF activated the complement cascade, with scFv-Fc-ΔXF inducing higher cell lysis compared to rituximab (Figure 5C). The activity of hIL-2 was assayed using a CTLL2 cell proliferation assay. As displayed in figure 6, both IC-ΔXF and IC induced higher cell proliferation compared to an equimolar concentration of recombinant human IL-2. As expected, scFv-Fc and scFv-Fc-ΔXF were not capable to induce any significant cell proliferation. Altogether these results confirm the whole biological integrity of the antibody (Fab and Fc functions) and cytokine components of both IC-ΔXF and IC.

4. Discussion

Immunocytokines based on recombinant scFv-Fc antibody format are an innovative class of biopharmaceuticals, being devised for targeted therapy of tumors. The advantage of these molecules is to combine the antibody effector functions with those of a cytokine that, being precisely targeted to the tumor, can be administered at lower doses, thus decreasing possible side effects and

improving the efficacy. In this study, we have assessed the influence of glycosylation on the biological activity of the plant-produced recombinant anti-CD20 immunocytokine, targeting non-Hodgkin's lymphoma. Fc glycosylation for therapeutic antibodies has a profound impact on the effector functions, such as ADCC and CDC, by affecting the interaction with Fc gamma receptors (FcγRs) and complement proteins, respectively (Jefferis, 2009). The immunocytokine (IC-ΔXF) as well as the scFv-Fc-ΔXF antibody were produced in glyco-modified plants lacking xylose and fucose sugars at yields (20-35 mg/Kg of FW) comparable to those previously reported in wild-type plants (Marusic et al., 2016). The protein profile was very similar to that previously described in literature (Marusic et al., 2016) and in particular there is no difference in band profiles and intensity between glycoengineered and non-glycoengineered molecules of the same format. IC-ΔXF and IC exhibited a slightly higher degradation compared to scFv-Fc and scFv-Fc-ΔXF antibodies with two products visible in the Coomassie-stained gel under non-reducing conditions, one at about 100kDa and the second at about 60 kDa. Although, it must be noted that size-exclusion chromatography analysis showed that about 90% of the purified immunocytokine was intact. Glycan analysis of both IC-ΔXF and scFv-Fc-ΔXF revealed the presence of a largely dominant glycoform $GlcNAc_2Man_3GlcNAc_2$, lacking xylose and fucose residues. In contrast, the different glycosylation had no impact on the antigen specificity since all glyco-variants bound CD20 on the surface of Daudi cells at comparable levels. This result was mostly expected since it was previously shown that a fucosyl-deprived anti-CD20 mAb retained full antigen binding activity (Chung et al., 2012). Also the IL2-dependent cell proliferation induced by IC-ΔXF and IC were comparable, indicating that the modified glycosylation profile has no effect on binding of the immunocytokine to IL2 receptors on CTLL cells. SPR binding analysis of IC-ΔXF to FcγRs showed that this glyco-modified immunocytokine had an enhanced binding if compared to IC with levels comparable to those of rituximab produced in CHO cells. Cell-surface FcγRI receptors expressed on monocytes, macrophages and dendritic cells, bind IgGs with high affinity and promote both innate and adaptive

immune responses (Bevaart et al., 2006; Kiyoshi et al., 2015). The importance of FcγRI in tumor therapy has also been discussed showing that neutrophils expressing this receptor participate in the anticancer activity of rituximab in a Non-Hodgkin's Lymphoma SCID (severe combined immunodeficiency) mouse model, by inducing ADCC (Hernandez-ilizaliturri et al., 2003). Recent studies pointed out the pivotal role of Fc glycan residues in IgG binding to FcγRI as antibody deglycosylation resulted in ~30-fold reduction. In particular, it was shown that the FcγRI FG-loop is involved in glycan recognition, making contacts with the proximal carbohydrate units (GlcNAc) of Fc glycans (Lu et al., 2015). Results here reported show that IC has a significantly lower affinity to FcγRI compared to that of the glyco-modified IC-ΔXF, indicating that either core xylose and/or fucose residues exert negative effects on FcγRI binding. SPR analysis of IC-ΔXF binding to the FcγRIIIa shows a 100-fold higher affinity compared to IC and ~10 fold higher affinity if compared to that of CHO-derived rituximab. This result was somehow expected in that removal of α1,6 fucose residues from CHO-derived rituximab has been already demonstrated to increase its affinity to FcγRIIIa by ~4 fold (Isoda et al., 2015). The higher affinity observed for the glyco-modified immunocytokine lacking core modifications indicates that α1,3 fucose and/or β1,2 xylose residues have a strong detrimental effect on the binding to FcγRIIIa. This result is in agreement with former studies on plant derived glyco-modified antibodies lacking xylose and fucose that showed a strong improvement (~10 fold) in FcγRIIIa binding (Jez et al., 2012; Cox et al., 2006). Moreover, we demonstrated that not only FcγRIIIa binding is enhanced by glyco-modification but also ADCC activity. In fact, both IC-ΔXF and scFv-Fc-ΔXF showed a strong ADCC activity with more than doubled cell lysis response if compared to those of their 'wild-type' glycosylated counterparts and that of the CHO-derived rituximab. To our knowledge, there are only few examples demonstrating the direct effect of glyco-engineering on the ADCC activity of plant-produced, tumor-targeting antibodies. Among them, the anti-CD30 human mAb developed for the treatment of Hodgkin lymphoma produced in glyco-engineered *Lemna minor*, lacking core α1,3 fucose and β1,2 xylose

glycans, showed a significantly increased ADCC activity if compared to both the 'wild-type' plant glycosylated and CHO-derived mAbs (Cox et al., 2006). Moreover, recombinant antibody fragments (Fcabs) targeting the human epidermal growth factor receptor 2 (HER2) had a 20-50 fold increase in ADCC activity if compared to the corresponding antibodies containing fucose residues (Jez et al., 2012). Overall, these results highlight that, regardless of the antibody format, plant-derived immunoglobulins lacking N-glycan core residues have significantly enhanced antibody-dependent cellular toxicity activity against human tumor cells, supporting the concept of tailoring glycan decoration on immunoglobulin scaffolds towards enhanced biological activity.

Intriguingly, we found that both recombinant molecules with typical plant glycans (IC and scFv-Fc) had low binding activity to the human complement component C1q, while the glyco-modified counterparts had binding activity similar to that of rituximab. The complement cascade is a complex system made up of more than 30 proteins and protein fragments, including C1q which, by binding to the Fc portion of IgGs, allows the activation of the "classical" (antibody-dependent) complement pathway (Meyer et al., 2014). Glycosylation of the antibody Fc is known to have some influence on C1q binding. Indeed, a fucosyl-deprived anti-CD20 antibody had a slight affinity improvement if compared to the fucosylated counterpart (Chung et al., 2012), while Fc sialylation of rituximab strongly impaired binding to C1q (Quast et al., 2015). It has also been reported that higher terminal galactose content of rituximab contributes to increased binding to C1q and consequently increased CDC (Hodoniczky et al., 2005). It was previously shown that plant-produced antibodies against West Nile Virus with different glycosylation patterns had different binding affinities to C1q, with the lowest associated to antibodies containing high percentages of GnGnXF sugars (He et al., 2014). Another work evaluated the binding to C1q of plant-produced glycan variants of a respiratory syncytial virus specific antibody evidencing that the antibody lacking core xylose and fucose sugars was able to bind to C1q even if at lower levels when compared to mammalian cell produced versions (Hiatt et al., 2014). An a-fucosylated version of rituximab obtained in a *Lemna*

aquatic plant-based system showed enhanced ADCC but lower CDC activity (Gasdaska et al., 2012). In our study, we observed an impairment of C1q binding of the antibodies with typical plant glycans, whereas the glyco-modified antibodies restored C1q recognition showing binding levels similar to those observed for rituximab. These data are in accordance with the observed capacity of the glyco-modified molecules (IC-ΔXF and scFv-Fc-ΔXF) to induce complement-dependent cytotoxicity (CDC) while IC and scFv-Fc showed no significant cell death. Modulation of the complement cascade through the modification of Fc glycosylation represents an interesting strategy for the improvement of tumor-targeting immunoglobulins. In fact, there is evidence suggesting that complement can be, in certain applications, detrimental in mAb therapy. In particular, it has been shown that the incubation of rituximab with complement-active serum, blocked the adhesion of NK cells *in vitro* via the FcγRIII leading to an impaired ADCC activity (Wang et al., 2008). Moreover, NK-mediated ADCC capacity of the glyco-engineered mAb obinutuzumab (GA101), showing a diminished ability to fix complement if compared to rituximab, was not influenced by the presence of complement (Kern et al., 2013). In addition, it was also demonstrated that patients homozygous for a single nucleotide polymorphism (SNP) in the C1qA gene that results in lower C1q levels (Gly70GGA) attained a extended remission when treated with rituximab monotherapy compared to heterozygous or homozygous G genotyped patients (Gly70GGG) (Racila et al., 2008).

In conclusion, we demonstrated that N-glycan modifications of the plant produced tumor-targeting anti-CD20 immunocytokine IC-ΔXF and the scFv-Fc-ΔXF recombinant antibody fragment enhanced their biological activity leading to a possible improvement of their therapeutic potential. Our study provides a detailed characterization of the impact of glycosylation on the effector functions of cancer-targeting recombinant immunocytokines produced in plant. In particular, we showed that plant-typical glycosylation has a negative impact in the binding to both FcγRI and FcγRIIIa and a negative effect on the activation of the complement cascade. The possibility of controlling antibody dependent cytotoxicity by modulating Fc glycosylation represents an

interesting perspective for the use of plant-made tumor-targeting immunoglobulins. Therefore, antibodies with plant typical glycans may serve to better understand the role of different glycan decoration in Fc receptor binding and to modulate specific immune effector functions, such as CDC, to potentiate immunotherapeutic applications. Future efforts will also be devoted to the evaluation of the therapeutic potential of the plant-produced glyco-engineered immunocytokine in tumour animal models.

Acknowledgments

We thank the Italian Ministry of Foreign Affairs,'Direzione Generale per la Promozione del Sistema Paese, Unita' per la cooperazione scientifica e tecnologica bilaterale e multilaterale'. We thank Prof. Herta Steinkellner for helpful discussion of the manuscript and for providing ΔXylT/FucT *N. benthamiana* seeds. We also thank Dr. Cristina Capodicasa for the control scFv-Fc antibody. Conflict of Interest Statement: A patent on the described glyco-engineered molecules in this manuscript was filed on 30/01/2017 at the Italian Patent Office (application 102017000009339).

References

Armitage JO, Gascoyne RD, Lunning MA, Cavalli F. 2017. Non-Hodgkin lymphoma. *Lancet* **390**:298–310.

Bevaart L, Jansen MJH, van Vugt MJ, Verbeek JS, van de Winkel JGJ, Leusen JHW. 2006. The high-affinity IgG receptor, FcgammaRI, plays a central role in antibody therapy of experimental melanoma. *Cancer Res.* **66**:1261–4.

Calcagno A, Rostagno R, Di Perri G. 2012. Anti-CD20 antibody therapy for B-cell lymphomas. *N. Engl. J. Med.* **367**:877–8; author reply 878.

Capodicasa C, Chiani P, Bromuro C, De Bernardis F, Catellani M, Palma AS, Liu Y, Feizi T, Cassone A, Benvenuto E, Torosantucci A. 2011. Plant production of anti-β-glucan antibodies for immunotherapy of fungal infections in humans. *Plant Biotechnol. J.* **9**:776–87.

Chung S, Quarmby V, Gao X, Ying Y, Lin L, Reed C, Fong C, Lau W, Qiu ZJ, Shen A, Vanderlaan M, Song A. 2012. Quantitative evaluation of fucose reducing effects in a humanized antibody on Fcγ receptor binding and antibody-dependent cell-mediated cytotoxicity activities. *MAbs* **4**:326–40.

Cox KM, Sterling JD, Regan JT, Gasdaska JR, Frantz KK, Peele CG, Black A, Passmore D, Moldovan-Loomis C, Srinivasan M, Cuison S, Cardarelli PM, Dickey LF. 2006. Glycan optimization of a human monoclonal antibody in the aquatic plant Lemna minor. *Nat. Biotechnol.* **24**:1591–7.

D'Ambrosio C, Arena S, Salzano AM, Renzone G, Ledda L, Scaloni A. 2008. A proteomic characterization of water buffalo milk fractions describing PTM of major species and the identification of minor components involved in nutrient delivery and defense against pathogens. *Proteomics* **8**:3657–66.

Davis BTA, Grillo-lo AJ, White CA, Mclaughlin P, Czuczman MS, Link BK, Maloney DG, Weaver RL, Rosenberg J, Levy R. 2014. Rituximab Anti-CD20 Monoclonal Antibody Therapy in Non-Hodgkin ' s Lymphoma : Safety and Efficacy of Re-treatment. *J. Clin. Oncol.* **18**:3135–3143.

Forthal DN, Gach JS, Landucci G, Jez J, Strasser R, Kunert R, Steinkellner H. 2010. Fc-glycosylation influences Fcγ receptor binding and cell-mediated anti-HIV activity of monoclonal antibody 2G12. *J. Immunol.* **185**:6876–82.

Fournier P, Aigner M, Schirrmacher V. 2011. Targeting of IL-2 and GM-CSF immunocytokines to a tumor vaccine leads to increased anti-tumor activity. *Int. J. Oncol.* **38**:1719–29.

Gasdaska JR, Sherwood S, Regan JT, Dickey LF. 2012. An afucosylated anti-CD20 monoclonal antibody with greater antibody-dependent cellular cytotoxicity and B-cell depletion and lower complement-dependent cytotoxicity than rituximab. *Mol. Immunol.* **50**:134–41.

Gubbels J a a, Gadbaw B, Buhtoiarov IN, Horibata S, Kapur AK, Patel D, Hank J a, Gillies SD, Sondel PM, Patankar MS, Connor J. 2011. Ab-IL2 fusion proteins mediate NK cell immune synapse formation by polarizing CD25 to the target cell-effector cell interface. *Cancer Immunol. Immunother.* **60**:1789–800.

He J, Lai H, Engle M, Gorlatov S, Gruber C, Steinkellner H, Diamond MS, Chen Q. 2014. Generation and analysis of novel plant-derived antibody-based therapeutic molecules against West Nile virus. *PLoS One* **9**:e93541.

Hernandez-ilizaliturri FJ, Jupudy V, Ostberg J, Oflazoglu E, Huberman A, Repasky E, Czuczman MS. 2003. Neutrophils Contribute to the Biological Antitumor Activity of Rituximab in a Non-Hodgkin â€^{TM} s Lymphoma Severe Combined Immunodeficiency Mouse Model Neutrophils

Contribute to the Biological Antitumor Activity of Rituximab in a Non-Hodgkin ' s Lymphoma Seve. *Clin. Cancer Res.* **9**:5866–5873.

Hiatt A, Bohorova N, Bohorov O, Goodman C, Kim D, Pauly MH, Velasco J, Whaley KJ, Piedra PA, Gilbert BE, Zeitlin L. 2014. Glycan variants of a respiratory syncytial virus antibody with enhanced effector function and in vivo efficacy. *Proc. Natl. Acad. Sci. U. S. A.* **111**:5992–7.

Hodoniczky J, Zheng YZ, James DC. 2005. Control of recombinant monoclonal antibody effector functions by Fc N-glycan remodeling in vitro. *Biotechnol. Prog.* **21**:1644–52.

Isoda Y, Yagi H, Satoh T, Shibata-Koyama M, Masuda K, Satoh M, Kato K, Iida S. 2015. Importance of the Side Chain at Position 296 of Antibody Fc in Interactions with FcγRIIIa and Other Fcγ Receptors. Ed. Joseph J Barchi. *PLoS One* **10**:e0140120.

Jahn T, Zuther M, Friedrichs B, Heuser C, Guhlke S, Abken H, Hombach A a. 2012. An IL12-IL2-antibody fusion protein targeting Hodgkin's lymphoma cells potentiates activation of NK and T cells for an anti-tumor attack. *PLoS One* **7**:e44482.

Jefferis R. 2009. Glycosylation as a strategy to improve antibody-based therapeutics. *Nat. Rev. Drug Discov.* **8**:226–234.

Jefferis R. 2012. Isotype and glycoform selection for antibody therapeutics. *Arch. Biochem. Biophys.* **526**:159–166.

Jez J, Antes B, Castilho A, Kainer M, Wiederkum S, Grass J, Rüker F, Woisetschläger M, Steinkellner H. 2012. Significant impact of single N-glycan residues on the biological activity of Fc-based antibody-like fragments. *J. Biol. Chem.* **287**:24313–9.

Kern DJ, James BR, Blackwell S, Gassner C, Klein C, Weiner GJ. 2013. GA101 induces NK-cell activation and antibody-dependent cellular cytotoxicity more effectively than rituximab when complement is present. *Leuk. Lymphoma* **54**:2500–5.

Kiyoshi M, Caaveiro JMM, Kawai T, Tashiro S, Ide T, Asaoka Y, Hatayama K, Tsumoto K. 2015. Structural basis for binding of human IgG1 to its high-affinity human receptor FcγRI. *Nat. Commun.* **6**:6866.

List T, Neri D. 2013. Immunocytokines: a review of molecules in clinical development for cancer therapy. *Clin. Pharmacol.* **5**:29–45.

Lombardi R, Villani ME, Di Carli M, Brunetti P, Benvenuto E, Donini M. 2010. Optimisation of the purification process of a tumour-targeting antibody produced in N. benthamiana using vacuum-agroinfiltration. *Transgenic Res.* **19**:1083–1097.

Lu J, Chu J, Zou Z, Hamacher NB, Rixon MW, Sun PD. 2015. Structure of FcγRI in complex with Fc reveals the importance of glycan recognition for high-affinity IgG binding. *Proc. Natl. Acad. Sci. U. S. A.* **112**:833–8.

Marusic C, Novelli F, Salzano AM, Scaloni A, Benvenuto E, Pioli C, Donini M. 2015. Production of an active anti-CD20-hIL-2 immunocytokine in Nicotiana benthamiana. *Plant Biotechnol. J.*

Meyer S, Leusen JHW, Boross P. 2014. Regulation of complement and modulation of its activity in monoclonal antibody therapy of cancer. *MAbs* **6**:1133–1144.

Perry AM, Diebold J, Nathwani BN, MacLennan KA, Muller-Hermelink HK, Bast M, Boilesen E, Armitage JO, Weisenburger DD. 2016. Non-Hodgkin lymphoma in the developing world: review of 4539 cases from the International Non-Hodgkin Lymphoma Classification Project. *Haematologica* **101**:1244–1250.

Pretto F, Elia G, Castioni N, Neri D. 2014. Preclinical evaluation of IL2-based immunocytokines supports their use in combination with dacarbazine, paclitaxel and TNF-based immunotherapy. *Cancer Immunol. Immunother.* **63**:901–10.

Qiu X, Wong G, Audet J, Bello A, Fernando L, Alimonti JB, Fausther-Bovendo H, Wei H, Aviles J, Hiatt E, Johnson A, Morton J, Swope K, Bohorov O, Bohorova N, Goodman C, Kim D, Pauly MH, Velasco J, Pettitt J, Olinger GG, Whaley K, Xu B, Strong JE, Zeitlin L, Kobinger GP. 2014. Reversion of advanced Ebola virus disease in nonhuman primates with ZMapp. *Nature* **514**:47–53.

Quast I, Keller CW, Maurer MA, Giddens JP, Tackenberg B, Wang LX, Münz C, Nimmerjahn F, Dalakas MC, Lünemann JD. 2015. Sialylation of IgG Fc domain impairs complement-dependent cytotoxicity. *J. Clin. Invest.* **125**:4160–4170.

Racila E, Link BK, Weng W-K, Witzig TE, Ansell S, Maurer MJ, Huang J, Dahle C, Halwani A, Levy R, Weiner GJ. 2008. A polymorphism in the complement component C1qA correlates with prolonged response following rituximab therapy of follicular lymphoma. *Clin. Cancer Res.* **14**:6697–703.

Reff ME, Carner K, Chambers KS, Chinn PC, Leonard JE, Raab R, Newman RA, Hanna N, Anderson DR. 1994. Depletion of B cells in vivo by a chimeric mouse human monoclonal antibody to CD20. *Blood* **83**:435–45.

Sawas A, Farber CM, Schreeder MT, Khalil MY, Mahadevan D, Deng C, Amengual JE, Nikolinakos PG, Kolesar JM, Kuhn JG, Sportelli P, Miskin HP, O'Connor OA. 2017. A phase 1/2 trial of ublituximab, a novel anti-CD20 monoclonal antibody, in patients with B-cell non-Hodgkin lymphoma or chronic lymphocytic leukaemia previously exposed to rituximab. *Br. J. Haematol.*:1–11.

Sondel PM, Gillies SD. 2012. Current and Potential Uses of Immunocytokines as Cancer Immunotherapy. *Antibodies* **1**:149–171.

Stoger E, Fischer R, Moloney M, Ma JK-C. 2014. Plant molecular pharming for the treatment of chronic and infectious diseases. *Annu. Rev. Plant Biol.* **65**:743–68.

Strasser R, Altmann F, Mach L, Glössl J, Steinkellner H. 2004. Generation of Arabidopsis thaliana plants with complex N-glycans lacking β1,2-linked xylose and core α1,3-linked fucose. *FEBS Lett.* **561**:132-6.

Strasser R, Altmann F, Steinkellner H. 2014. Controlled glycosylation of plant-produced recombinant proteins. *Curr. Opin. Biotechnol.* **30**:95–100.

Strasser R, Stadlmann J, Schähs M, Stiegler G, Quendler H, Mach L, Glössl J, Weterings K, Pabst M, Steinkellner H. 2008. Generation of glyco-engineered Nicotiana benthamiana for the production of monoclonal antibodies with a homogeneous human-like N-glycan structure. *Plant Biotechnol. J.* **6**:392–402.

Villani ME, Morgun B, Brunetti P, Marusic C, Lombardi R, Pisoni I, Bacci C, Desiderio A, Benvenuto E, Donini M. 2009. Plant pharming of a full-sized, tumour-targeting antibody using different expression strategies. *Plant Biotechnol. J.* **7**:59–72.

Vincent M, Teppaz G, Lajoie L, Solé V, Bessard A, Maillasson M, Loisel S, Béchard D, Clémenceau B, Thibault G, Garrigue-Antar L, Jacques Y, Quéméner A. 2014. Highly potent anti-CD20-RLI immunocytokine targeting established human B lymphoma in SCID mouse. *MAbs* **6**:1026–37.

Wang S-Y, Racila E, Taylor RP, Weiner GJ. 2008. NK-cell activation and antibody-dependent cellular cytotoxicity induced by rituximab-coated target cells is inhibited by the C3b component of complement. *Blood* **111**:1456–63.

Tables and Figures Captions

Table 1. Kinetics and affinity parameters for the interaction of FcγRI with IC, IC-ΔXF and rituximab. Half-life of the immunocytokine-receptor complex as calculated from the dissociation rate constant (k_{off}). Rmax denotes a maximum response upon saturation. Chi^2 represents an average deviation of the fitted model from the experimental data. Deviations lower than 5% of the Rmax indicate a good fit.

Table 2. Kinetics and affinity parameters for the interaction of FcγRIIIa with the immunocytokine. The Two-state binding model provides two sets of kinetics values for the 1^{st} and 2^{nd} step of binding process respectively, which translate to a single affinity value. Kinetics and affinity to the 'wild-type' plant glycosylated IC could not be precisely determined.

Figure 1. Characterization of glyco-engineered anti-CD20 immunocytokine

(A) Coomassie-stained non-reducing SDS-10% PAGE analysis of purified IC-ΔXF and IC (lanes 2 and 3, respectively); scFv-Fc-ΔXF and scFv-Fc (lanes 4 and 5, respectively) and the control rituximab produced in CHO cells (lane 1). One μg of protein was loaded in each lane; M: marker for protein molecular mass. (B) Typical Coomassie-stained reducing SDS-10% PAGE analysis of purified scFv-Fc-ΔXF and IC-ΔXF. (C) Size exclusion chromatography of purified recombinant molecules was performed using a Superdex^{TM} 200 column. Top panel represents the chromatogram obtained for CHO derived rituximab (RTX); retention volumes (ml) of chromatographic peaks are reported as well as the percentages of the area of the major peaks. (D) Anti-hIL-2 ELISA. The ELISA plate coated with an anti-human-γ chain antibody and 10 ng of purified proteins were added before detection with an anti-hIL-2 antibody; scFv-Fc-ΔXF and PBS represent the negative controls. Values represent the mean of three independent experiments; error bars are SD of the means.

Figure 2. N-glycan analysis.

MALDI-TOF-MS analysis of the glycopeptide EEQYNSTYR (339-347) containing various complex-type N-linked glycan structures. Trapping on HILIC resin allowed the recovery of glycopeptide products from the digests obtained following treatment of scFv-Fc (A), scFv-Fc-ΔXF (B) and IC-ΔXF (C) with trypsin. In the spectra mass signals not associable to glycopeptide species are not labelled.

Figure 3. FcγR binding studies by SPR measurements.

SPR sensorgrams demonstrating binding and dissociation patterns for FcγRI (A) and FcγRIIIa (B) interaction with rituximab, IC and IC-ΔXF. The Langmuir (1:1) binding model (black lines) was fitted to the experimental data (coloured lines) for FcγRI (A) while the 'Two-state reaction' binding model was used for FcγRIIIa (B). Different curves correspond to FcγRI concentrations of 30 nM,

15 nM, 7.5 nM, 3.75 nM and 1.88 nM and to FcγRIIIa concentrations of 2 μM, 1 μM, 0.5 μM, 0.25 nM and 0.125 μM for rituximab and IC, and 800 nM, 400 nM, 200 nM, 100nM, 50 nM, 25 nM, 12.5 nM for IC-ΔXF. RU: Resonance Units.

Figure 4. Antigen (CD20) binding studies.

Flow cytometry analysis of $CD20^+$ Daudi cells labeled with rituximab, IC, IC-ΔXF, scFv-Fc or scFv-Fc-ΔXF. Binding of the molecules to CD20 was assayed using a goat anti-human IgG polyclonal Ab and detected with a FITC-conjugated Ab. Values represent mean ± S.E of percentages of positive cells. Data was obtained from three independent experiments. As a negative control (Ctrl), the plant-derived anti-tenascin C mAbH10 was used.

Figure 5. Studies of Fc mediated effector functions.

(A) Antibody-dependent cell-mediated cytotoxicity. The different molecules (rituximab, IC, IC-ΔXF, scFv-Fc or scFv-Fc-ΔXF) were added to Daudi cells cultured with IL-2-activated human PBMCs. LDH release was used to evaluate the percentage of cytotoxicity. Results shown are means of two independent experiments ± S.E. *, $p < 0.05$ for scFv-Fc-ΔXF and IC-ΔXF compared to rituximab, scFv-Fc and IC. (B) Binding to C1q was assayed by anti-C1q ELISA. Plates were coated with recombinant IC, IC-ΔXF, scFv-Fc, scFv-Fc-ΔXF and rituximab at serial dilutions (starting from 10 μg/ml). Purified C1q followed by an HRP conjugated anti-C1q antibody was then added to the plate. Values represent the mean of triplicate samples ± SE. (C) Effects of glyco-engineering on the Complement Dependent Cell Cytotoxicity (CDC) activity. Daudi cells were incubated with different concentrations of IC, IC-ΔXF, scFv-Fc, scFv-Fc-ΔXF and rituximab in the presence of human serum and analyzed by flow cytometry. Necrotic cells were detected using propidium iodide staining. As a control, Daudi cells were incubated either with the recombinant molecules without serum or with serum alone, showing no detectable cell death (not shown). Results shown are means

of two independent experiments ± S.E. *, $p < 0.05$ for scFv-Fc-ΔXF compared to scFv-Fc; **, $p < 0.05$ for IC-ΔXF compared to IC; §, $p < 0.05$ for rituximab compared to scFv-Fc, IC and IC-ΔXF.

Figure 6. **IL2 activity assessments.**

CTLL-2 cells were cultured with complete medium only or stimulated with 160 nM of rhIL2, IC-ΔXF or IC. scFv-Fc-ΔXF and scFv-Fc were used as controls. MTS to formazan reduction assay was used to evaluate cell proliferation indicated as absorbance values (O.D. 490 nm). Values are mean ± S.D. of triplicate cell cultures. *, $p<0.05$ for IC-ΔXF and IC versus scFv-Fc-ΔXF, scFv-Fc and rhIL2 (One way ANOVA plus post hoc Bonferroni-corrected two-tailed student's t-test).

Supplementary figure S1

MALDI LIFT-TOF/TOF-MS spectrum of the glycopeptide EEQYNSTYR (339-347) at *m/z* 2487.9. The y and b series peptide fragments are shown. The deglycosylated peptide corresponding to the signal doublet is indicated by the asterisk. The ring fragmentation signal of the innermost GlcNAc is reported as 0.2 X; a. u.: arbitrary units

Table 1. Kinetics and affinity parameters for the interaction of FcγRI with IC, IC-ΔXF and rituximab. Half-life of the immunocytokine-receptor complex as calculated from the dissociation rate constant (k_{off}). Rmax denotes a maximum response upon saturation. Chi^2 represents an average deviation of the fitted model from the experimental data. Deviations lower than 5% of the Rmax indicate a good fit.

Antibody	**k_{on} (10^6 M^{-1} s^{-1})**	**k_{off} (10^{-4} s^{-1})**	**half life (min)**	**K_D**	**Rmax (RU)**	**Chi^2 (RU^2)**	**Closeness of fit**
Rituximab	1.84	6.09	19	332 pM	55	1.76	3.2%
IC	1.19	34.4	3.4	2.9 nM	67	1.49	2.2%
IC-ΔXF	1.88	2.8	61.5	150 pM	99	1.48	1.5%

Table 2. Kinetics and affinity parameters for the interaction of FcγRIIIa with the immunocytokines. The Two-state binding model provides two sets of kinetics values for the 1st and 2nd step of binding process respectively, which translate to a single affinity value. Kinetics and affinity to the 'wild-type' plant glycosylated IC could not be precisely determined.

Antibody	**$k_{on}1$ (10^5 M^{-1} s^{-1})**	**$k_{off}1$ (s^{-1})**	**$k_{on}2$ (10^{-3} s^{-1})**	**$k_{off}2$ (10^{-2} s^{-1})**	**K_D**
Rituximab	14.5	0.76	7.96	2.1	377 nM
IC	-	-	-	-	> 2 μM
IC-ΔXF	5.8	0.02	4.1	0.8	23.6 nM

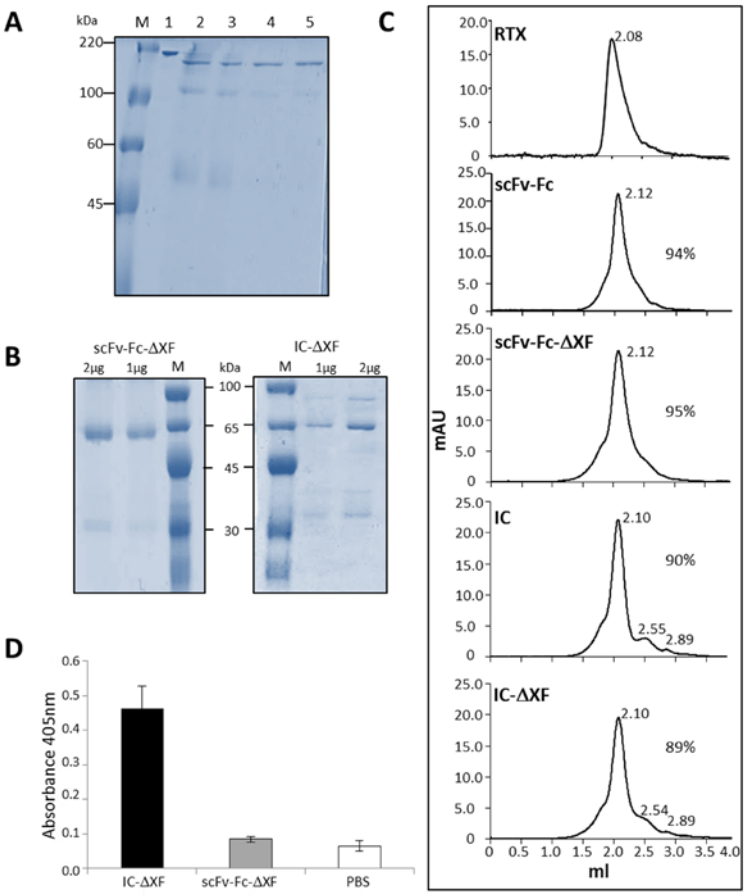

Figure 1

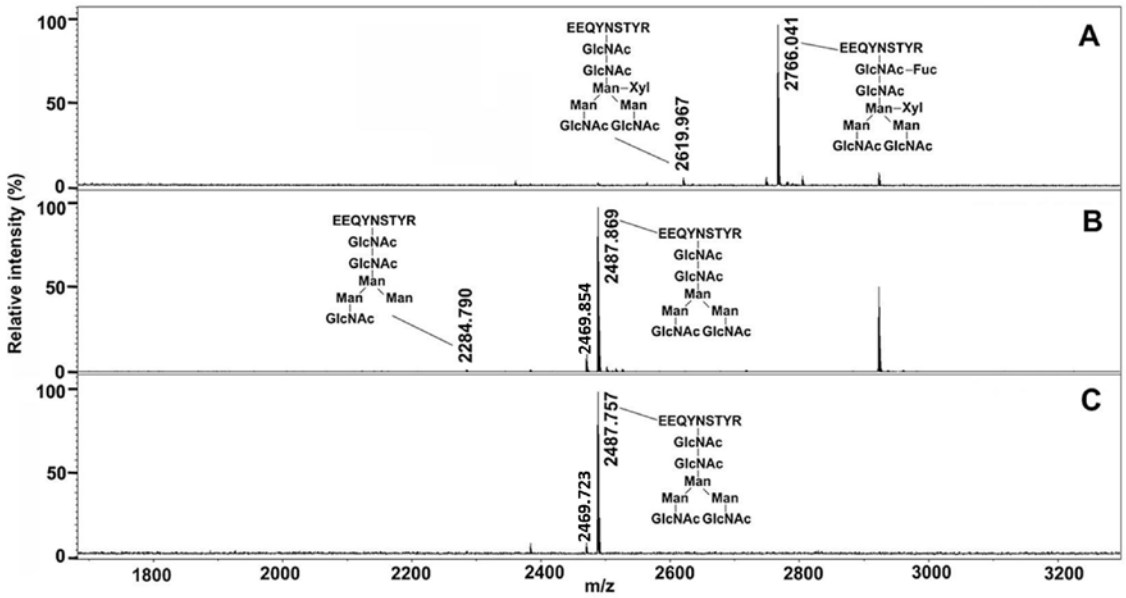

Figure 2

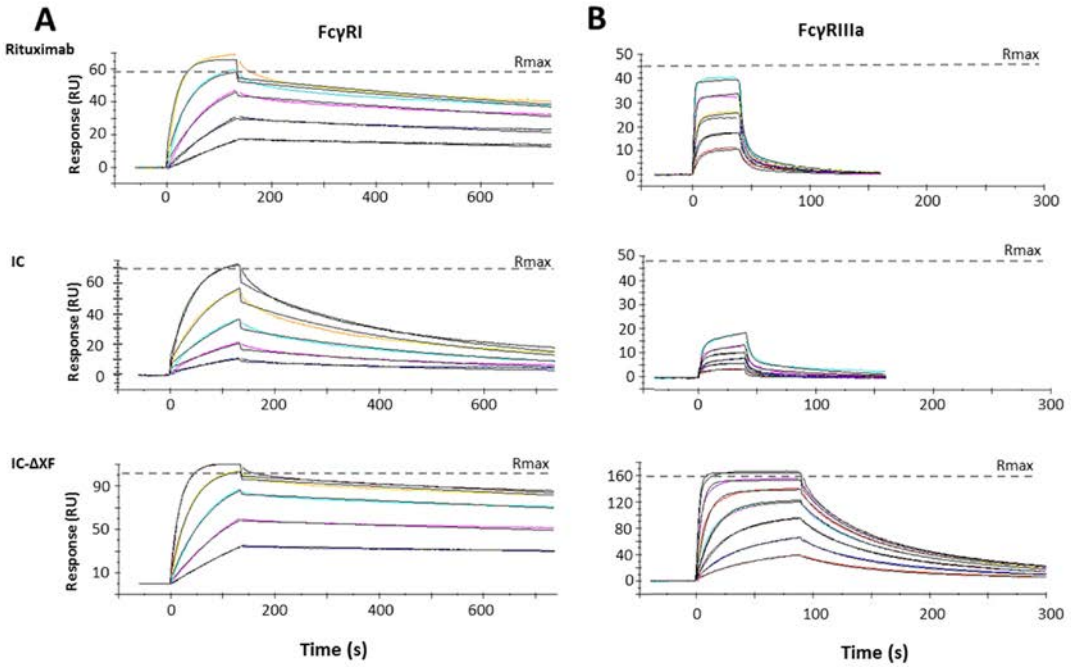

Figure 3

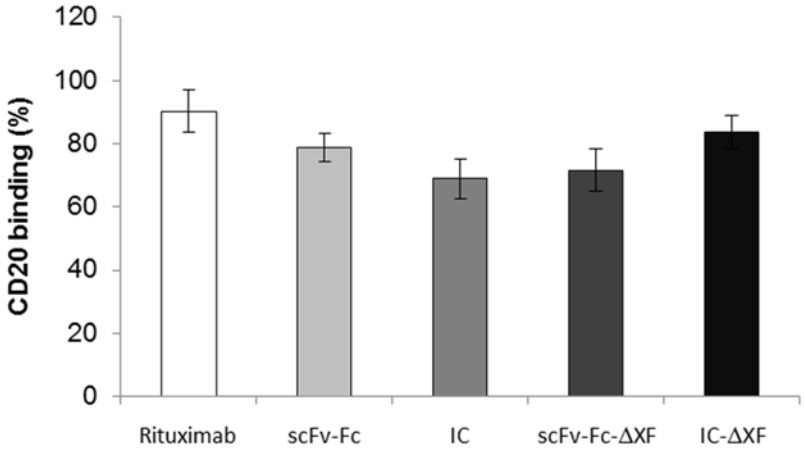

Figure 4

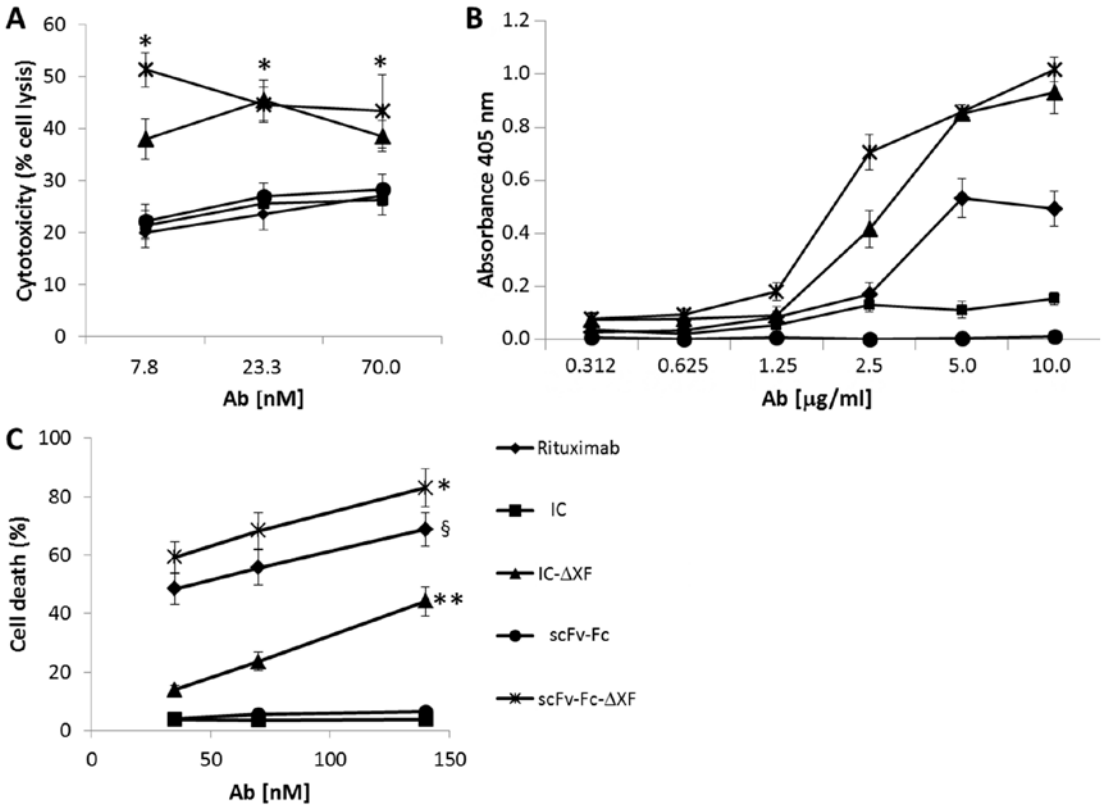

Figure 5

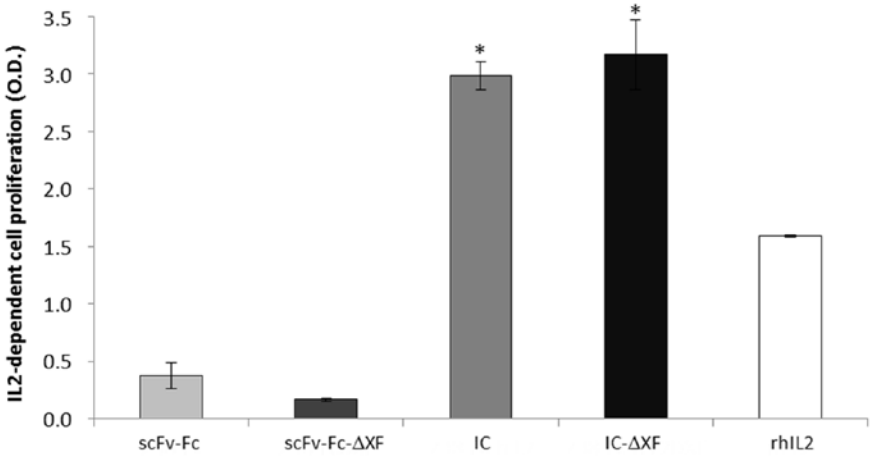

Figure 6